JOURNAL OF CATALYSIS 95, 353–360 (1985)

The Synthesis of Platinum Metal Alloys by a Precipitation Method

A. J. S. CHOWDHURY,* A. K. CHEETHAM,* AND J. A. CAIRNS†

*Chemical Crystallography Laboratory, University of Oxford, 9 Parks Road, Oxford OX1 3PD, †Engineering Sciences Division, Atomic Energy Research Establishment, Harwell, Didcot, Oxfordshire OX11 0RA, England

Received August 8, 1984; revised April 18, 1985

A method for the preparation of Pt–Ru, Pt–Rh, and Pt–Pd alloys by low-temperature, chemical routes has been described. The method involves two steps: first, the rapid precipitation of sulphides from a mixed aqueous solution by H_2S gas and, second, the reduction of the precipitate at a low temperature by hydrogen. The phase diagram of Pt–Ru has been studied at 650°C; its oxidation behaviour has also been investigated. The Pt–Rh alloys prepared at 700°C oxidise at low temperature (500°C) to Pt metal and Rh_2O_3; the oxide starts to decompose from about 800°C and at 1000°C the alloy is formed again. The decomposition temperature of Rh_2O_3 is lowered in the presence of Pt due to the free energy of formation of the alloy. © 1985 Academic Press, Inc.

INTRODUCTION

Preparations of finely powdered metals and alloys have been carried out by many methods of which the following three are the most widely used in catalytic work: the Adams method (*1*), the borohydride method (*2*), and the method of direct reduction of single or mixed metal hydroxides or oxides (*3*). With the exception of the borohydride reaction, these methods involve the reduction of intermediate oxides using hydrogen. In this paper we present a method for the preparation of homogeneous platinum metal alloys by a route involving the precipitation of sulphides from aqueous solutions. The method is derived from reactions that have been used to prepare refractory alloys by simple, low-temperature routes (*4*, *5*).

The method involves two separate steps: (i) rapid precipitation of insoluble compounds from aqueous solutions containing the elements in question; and (ii) reduction of the precipitate under flowing hydrogen at low temperatures. The success of the method hinges upon finding a suitable precipitant and the correct reaction conditions, so that a homogeneous precipitate is obtained prior to reduction.

For the platinum metal alloys, we have used hydrogen sulphide gas to precipitate the metals as their corresponding sulphides. This route is clearly appropriate for the late transition and posttransition metals which form very insoluble sulphides, but is unsuitable for more electropositive elements. The alloys prepared in this work are Pt–Ru, Pt–Rh, and Pt–Pd.

The Pt–Ru phase diagram contains two phases, an fcc Pt-rich phase and an hcp Ru-rich phase. The most recent studies indicate that the miscibility gap is from 62 to 69 at.% Ru at 700°C (*6*), or from 60 to 90 at.% Ru at 1000°C (*7*). In contrast, the Pt–Rh and Pt–Pd phase diagrams reveal complete miscibility between the fcc metals (*8*, *9*).

These alloys are of interest in a wide range of catalytic reactions, for example, in three-way catalytic converters (*10*), and we have studied two aspects of our powdered alloys that have a bearing on their catalytic behaviour, namely their morphology and their reactivity under oxidising conditions.

EXPERIMENTAL

Preparation

Pt–Ru alloys. Appropriate quantities of

0021-9517/85 $3.00

$H_2PtCl_6 \cdot 6H_2O$ and $RuCl_3 \cdot 3H_2O$ were dissolved separately in water giving solutions with pH 5–6. The solutions were mixed together and H_2S was passed slowly for 5–10 min during which the solution was stirred continuously. The precipitation starts slowly, but is complete within a few hours. Sometimes the solution was left undisturbed overnight to allow the fine precipitate to settle, leaving a colourless supernatant solution; the starting solution was dark brown. The precipitate was washed with water several times, dried, and ground to a fine powder. It was examined at this stage by electron microscopy and X-ray powder diffraction to assess its homogeneity and crystallinity. Reduction was carried out at 650°C under hydrogen for 5–6 h. Alloys were prepared from solutions with the following compositions (Ru + Pt = 100 at.%): 17.3, 38.1, 52.3, 65.9, 68.9, 77.6, and 93.5 at.% Ru. In order to complete the phase diagram, pure Pt and pure Ru were also prepared by the same method.

Pt–Rh alloy. The platinum–rhodium alloy was prepared from a mixed aqueous solution of $RhCl_3 \cdot 3H_2O$ and $H_2PtCl_6 \cdot 6H_2O$, as described above. Hydrogen reduction was carried out at 700°C for 24 h (alloys prepared at 600 and 650°C were contaminated with residual sulphur). Since the phase diagram is well established, a large sample of a single composition (starting solution containing 66.3 at.% Rh) was prepared.

Pt–Pd alloys. These alloys were prepared by precipitating the sulphides from the aqueous solutions of K_2PdCl_4 and $H_2PtCl_6 \cdot 6H_2O$. The hydrogen reduction was carried out at 800°C for 5–6 h (reductions carried out at 550 or 600°C may be contaminated with sulphur). For all the Pt–Pd alloys, it was necessary to heat the samples under vacuum for 2–3 h at 500°C to remove any residual hydrogen. The compositions of the starting solutions of the Pt–Pd alloys were 32.8, 47.8, 63.9, 79.9, and 86.3 at.% Pd. Pure palladium was also prepared by the same method.

Characterisation

The precipitates and alloys were characterised primarily by electron microscopy and X-ray powder diffraction measurements. The surface area of one of the Pt–Ru alloys was measured by the BET method.

Electron microscopy. The electron optical analyses were carried out using a JEOL 100CX TEMSCAN analytical electron microscope which provides the facilities of TEM, SEM, and X-ray microanalysis. To ascertain the compositions of the alloys by microanalysis the ratio method was used (*11, 12*) with proportionality constants, *k*, determined from homogeneous monophasic alloys of known compositions. Approximately 20 individual particles of each sample were analysed. The method was particularly useful for assessing the homogeneity and crystallinity of the precipitates.

X-Ray diffraction. The X-ray powder diffraction patterns of the Pt–Ru alloys were measured by a Guinier–Hägg camera and those of Pt–Rh and Pt–Pd alloys by a Guinier–Stoe camera; the lines tended to be rather broad. The precipitates themselves were amorphous.

RESULTS

Pt–Ru Alloys

The X-ray diffraction patterns clearly showed that the samples up to 38 at.% Ru were monophasic solid solutions of Ru in Pt. Above 80% Ru the alloys were hexagonal solid solutions, and between 52 and 77.6 at.% Ru they were biphasic. The lattice parameters of the fcc alloy decreased from 3.919 Å for pure Pt to approximately 3.85 Å at the phase limit. The volume of hcp Ru-rich phase increased as Pt was added (see Table 1). The sample at 52.3 at.% Ru was somewhat puzzling; the fcc lines were very faint, only two lines were visible, not sufficient for lattice parameter calculation, and the hexagonal cell volume was unexpectedly large. The result was reproducible,

TABLE 1

Cell Volumes and Lattice Parameters of Pt–Ru Alloys

Composition of the starting solution (Pt + Ru = 100 at.%) (at.% Ru)	Cell volumes (Å^3)		Lattice parameters (Å)	
	Cubic phase	Hexagonal phase	Cubic phase	Hexagonal phase
0	60.2		3.919(1)	
17.3	59.3		3.900(3)	
38.1	58.6		3.885(1)	
52.3	[a]	28.0	[a]	a_0 2.714(1) c_0 4.386(1)
65.9	56.8	27.7	3.843(3)	a_0 2.718(2) c_0 4.325(5)
77.7	57.3	27.6	3.854(4)	a_0 2.718(1) c_0 4.312(2)
93.5		27.1		a_0 2.702(1) c_0 4.288(4)
100		27.2		a_0 2.709(1) c_0 4.288(1)

[a] Only two reflections were visible, not sufficient for lattice parameter calculation.

suggesting that a metastable hcp phase was forming.

Microanalysis of the alloys was carried out with well-formed particles 400–700 Å in diameter (Fig. 1). The intermediate sulphides, which were very beam-sensitive, were agglomerates of many smaller particles. To ascertain the compositions of the alloys, the proportionality constant *k* was determined from the 17% Ru alloy which was monophasic and homogeneous. Using the (Pt*Lα*)/(Ru*Kα*) ratio, the *k* value was found to be 0.31. The compositions of the monophasic alloys were obtained using this *k* value and are presented in Table 2. The alloys with nominal compositions of 65.9, 68.9, and 77.6 at.% Ru gave the phase boundary of the fcc solid solution as 65.2, 62.0, and 68.4 at.% Ru, respectively, and the corresponding values for the hcp limit were 73.0, 80.0, and 86.6 at.% Ru.

TABLE 2

Compositions of the Pt–Ru Alloys and Precipitates from Microanalysis

Composition of the starting solution (at.% Ru)	Composition of the sulphide precipitate (at.% Ru)	Composition of the alloy (at.% Ru)
17.3	15.8	17.3
38.1	37.7	38.1
52.3	51.2	Biphasic
65.9	62.6	Biphasic
68.9	66.5	Biphasic
77.6	66.7	Biphasic
93.5	95.5	95.4

Measurement of surface area. The surface area of the 65.9 at.% Ru alloy was found to be 8.4 m^2/g, measured by the BET method. The surface area remained constant after annealing the alloy for a further 17 h at 650°C.

Oxidation behavior of Pt–Ru alloy. Two fresh samples of compositions 16.9 and 33.3 at.% Ru were heated in air for 4 h at temperatures ranging from 600 to 1000°C. Loss of weight was observed and the lattice parameter of the fcc phase increased as the decomposition temperature was increased. The presence of RuO_2 as an intermediate was noticeable above 600°C. Microanalysis and the lattice parameter of the fcc phase (3.92 Å) at 1000°C confirmed that all the Ru from the 16.9 at.% sample had volatilised (as RuO_4) at 1000°C. The line broadening by the fcc phase was exhibited at 800°C, the temperature at which the RuO_2 component was most apparent. This may be due to a

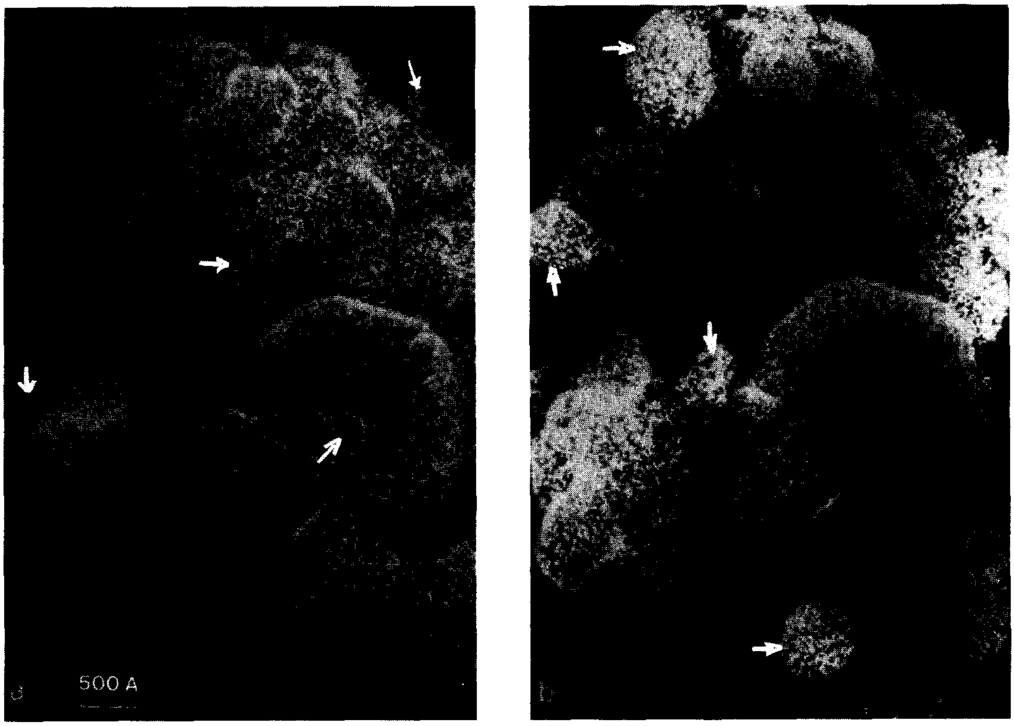

FIG. 1. Elemental maps of Pt/Ru alloys: (a) Pt*Mα* map of 52.3 at.% Ru alloy showing crystals of both phases (Pt-rich crystals shown by arrows), (b) Ru*Lα* map of the same crystals (Ru-rich crystals shown by arrows).

reduction in particle size as the RuO_2 separates from the alloy, or it may stem from inhomogeneity arising from this process. The 33.3% Ru alloy also exhibited similar behaviour; a large shift in the lattice parameter of the fcc phase was noticed, but RuO_2 was still present after heating for 4 h at 1000°C.

Pt–Rh Alloys

The alloy and the precipitate were analysed both by microanalysis and X-ray diffraction. The lattice parameter of the alloy was 3.84 Å, very close to the expected value at this composition calculated by Végard's law (using 3.919 Å (Pt) and 3.80 Å (Rh), as found in the present work). The lattice parameter confirmed the composition of the alloy to be 66 ± 2 at.% Rh.

Oxidation behaviour of Pt–Rh alloy. Samples of the alloy were heated in air at temperatures in the range of 500 to 1100°C for 20–24 h and then cooled in air.

The X-ray diffraction results for the products and also for the pure alloy are shown in Table 3. The observations are summarised below:

TABLE 3

Lattice Parameters of Pure Pt–Rh alloy and the Products Obtained by Heating the Alloy in Air

Decomposition temperature (°C)	Lattice parameter (Å)		
	Pt (fcc)	Pt–Rh alloy phase	Rh_2O_3
(Pure alloy)	Absent	3.84(1)	Absent
500	Absent	3.86(1)	Absent
600	3.91(1)	3.85(1)	Present
700	3.92(1)	—	Present
800	3.92(1)	3.86(1)	Present
900	3.88(1)	3.84(1)	Present
1000	Absent	3.85(1)	Absent
1100	Absent	3.87(1)	Absent

(1) The Pt–Rh alloy annealed at 500°C apparently remained unchanged.

(2) Rhodium began to oxidise at 600°C and the presence of pure Pt, the oxide phase Rh_2O_3, and lines from the Pt–Rh alloy could be seen. At this temperature, Rh_2O_3 was present as a mixture of its hexagonal and orthorhombic phases.

(3) The optimum temperature for the formation of Rh_2O_3 was 700°C. At this temperature the product was a mixture of pure platinum and both forms of Rh_2O_3.

(4) At 800°C, the rhodium oxide began to decompose and some alloying with platinum was apparent. The powder pattern was very similar to that obtained for the sample annealed at 600°C.

(5) At 900°C, the presence of Pt, Rh_2O_3, and Pt–Rh alloy was also observed.

(6) Above 1000°C, the oxide fully decomposed and pure alloy was formed once more.

(7) The lattice parameter of the alloy heated at 1100°C was slightly larger than that observed at 1000°C. This may be due to a change in particle size which was suggested by the sharpening of the X-ray reflections.

In the absence of platinum, Rh powder heated at 600°C gives Rh_2O_3 rather slowly, but at 1000°C, its formation is rapid. Above 1100°C, Rh_2O_3 decomposes to rhodium metal in air (*13*). The lower decomposition temperature in the present work presumably arises from the free energy of formation of the Pt/Rh alloy.

The effect of heating the alloys in air as observed from the X-ray diffraction patterns is summarised in the flow chart:

$$\begin{tikzcd}
\text{Pt–Rh alloy} \arrow[r, "500^\circ\text{C}"'] & \text{Pt–Rh} \arrow[r, "600^\circ\text{C}"'] & \text{Pt} + \text{Pt–Rh} + Rh_2O_3 \arrow[d, "700^\circ\text{C}"] \\
 & & \text{Pt} + Rh_2O_3 \arrow[d, "800^\circ\text{C}"] \\
\text{Pt–Rh} & \text{Pt–Rh} \arrow[l, "1000^\circ\text{C}"] & \text{Pt} + \text{Pt–Rh} + Rh_2O_3 \arrow[l, "900^\circ\text{C}"]
\end{tikzcd}$$

The microanalysis results on the quenched samples were interesting. At 500°C, although there was no indication of phase separation in the Guinier patterns, the microanalysis of the small crystallites revealed inhomogeneity of the alloy crystals. At 600°C, crystals of various Pt–Rh alloy compositions as well as pure Pt and Rh_2O_3 were observed. At 700°C, although the X-ray pattern revealed only Pt and Rh_2O_3, some of the small crystallites still showed the presence of both Pt and Rh. This may be due to the formation of Rh_2O_3 on the surface of Pt crystals, as observed by Schmidt *et al.* (*14*). At 800 and 900°C, microanalysis was consistent with the presence of three phases, Pt, Pt–Rh, and Rh_2O_3, in agreement with the X-ray findings.

TABLE 4

Compositions and Lattice Parameters of the Pt–Pd Alloys

Compositions of the starting solutions in at.% Pd	Compositions of the alloys from electron microscopic analyses $\left(k\frac{\text{Pd}L\alpha}{\text{Pt}L\alpha} = 1\right)$	Lattice parameters of the alloys (Å)
		3.919(1) (Pure Pt)
32.8	33.5	3.905(2)
47.8	45.5	3.894(1)
63.9	63.9	3.884(1)
79.9	80.1	3.875(1)
86.3	92.3	3.869(1)
		3.864(1) (Pure Pd)

Pt–Pd Alloys

The alloys were analysed as before by analytical electron microscopy and their compositions agree well with the initial compositions of the starting solutions (Table 4). The homogeneity of the precipitate was good. The compositions of the alloys were calculated from the (Pd$L\alpha$)/(Pt$L\alpha$) ratio taking the proportionality constant as unity, as calculated from 63.9 at.% Pd alloy. The PdL line is a triplet, which was resolved by a least-squares fit programme to obtain the area of the Pd$L\alpha$ peak.[1]

The results obtained from the X-ray powder diffraction were surprising in that all the lattice parameters were considerably smaller than the expected values. The lattice parameter of the pure Pd was 3.864 Å instead of 3.890 Å.

DISCUSSION

The main finding from this work is that finely divided, but apparently homogeneous alloys can be synthesised by a precipitation method involving sulphides. X-Ray powder diffraction and analytical electron microscopy played important roles in the characterisation of the alloys and the precipitates. Figure 2 shows two X-ray emission spectra of a sulphide and its corresponding reduced product, the alloy. The disappearance of the S$K\alpha,\beta$ peak proved to be a simple method of confirming whether the reduction was complete. As the homogeneity of the precipitate is one of the main prerequisites of a homogeneous alloy preparation, careful analysis at this stage is important.

In Pt–Ru alloys, our results confirmed that the phases were essentially the same as those obtained by other methods. The finely divided nature of the products was clearly demonstrated by the SEM studies and surface area measurements; particle sizes were in the region of 600 Å for monophasic regions, but only about 400 Å for biphasic samples, presumably because of the slow diffusion and phase separation in these samples. Furthermore, it was shown that the compositions of the alloys were determined by the compositions of the initial aqueous solutions.

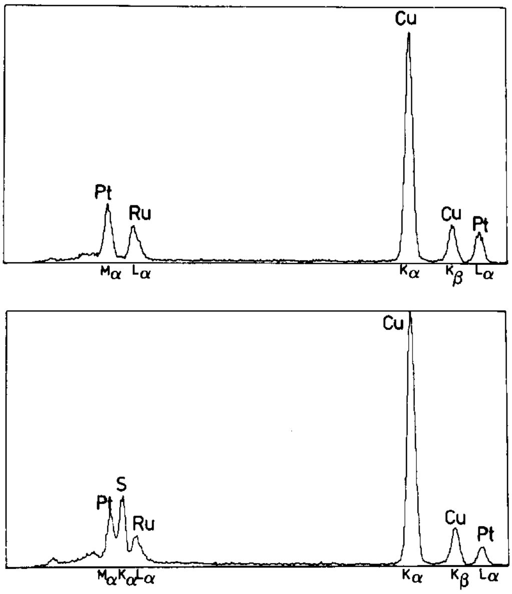

FIG. 2. X-Ray emission spectra (0–10 keV) of (below) Pt–Ru sulphide precipitate and (above) Pt–Ru alloy; composition 38.1 at.% Ru. The copper peak arises from the supporting grid.

The phase limit of the fcc solid solution was 60–65 at.% Ru according to the lattice parameter results, although the sample at 52.3 at.% Ru gave anomalous but reproducible results with the fcc phase hardly discernible and an hcp phase with a large cell volume. The X-ray emission analysis indicated a phase limit between 62 and 68.4 at.% Ru. The results for the fcc phase at 650°C were in good agreement with those obtained by others using different preparative methods (*6, 7*); the results of Bouwman and Sachtler (*15*) and the reported results from Battelle Memorial Institute (*16*) appeared anomalous with a solubility limit of only 50 Ru and 32 at.% Ru, respectively. The solubility limit of the hcp phase found in the present work indicated that about 15–20% Pt can be dissolved in the Ru lattice.

The microscopic examinations revealed that particles of both phases coexist together in the biphasic region and neither of these phases overlapped the other at any

---

[1] Least-squares curve-fitting programme, REFIN, which exists in the Chemical Crystallography Laboratory in Oxford.

stage; thus they did not show a constant surface composition over the entire miscibility gap. This was also observed by Bouwman and Sachtler (*15*). The equilibrium model proposed for Cu–Ni (*17*) and Pt–Au (*18*) alloys, where it has been shown that the Cu-phase covers the Ni, and the Au-rich phase covers the Pt-rich phase, does not apply in the case of Pt–Ru alloys.

The oxidation behaviour of Pt–Ru alloy demonstrated one further point: the loss of Ru at higher temperatures is inevitable and it is unsuitable for use as a commercial catalyst in the automobile catalytic converter, where prolonged use of such a catalyst will remove all the Ru as RuO_4.

The evidence obtained from the oxidation–reduction behaviour of Pt–Rh alloy indicated that the alloy was thermodynamically unstable with respect to oxidation at temperatures below about 800°C. However, the kinetics of the process were apparently slow below 600°C where the first appearance of Rh_2O_3 was observed. On further heating at 1000°C, the Rh_2O_3 was finally lost as it decomposed to rhodium and oxygen. This decomposition took place at a lower temperature in the presence of platinum because of the formation of Pt–Rh alloy.

From the known thermodynamic data of Rh_2O_3 (*19*), we have calculated the ΔG_f° of Rh_2O_3 at 900°C to be approximately −50 kJ/mole. The free energy of formation of the alloy $PtRh_2$, formed by the reaction

$$2Rh_2O_3 + 2Pt \rightarrow 2PtRh_2 + 3O_2,$$

is therefore approximately −50 kJ/mole at 900°C. The present findings and other published results indicate a delicate balance between the oxidation and decomposition behaviour of Rh_2O_3 in the presence of platinum. This might help to understand the catalytic behaviour observed in some reactions involving Pt–Rh alloys.

The Pt–Pd alloys are interesting in that although they can be prepared by the sulphide precipitation method, they reveal lattice contractions, particularly at the Pd-rich end. The lattice parameters of the present alloys obey Végard's law. The explanations for lattice contractions of microcrystals in terms of surface stress (*20*) and other models (*21, 22*) do not apply to the Pt–Pd alloys because the particle size is too large, and indeed larger than we observe in other alloys. The alloys do not show any appreciable tendency to form hydrides under the condition of our preparation and the lattice parameters are clearly too small for hydrides. The reason for the contraction is still unclear.

The intermediate sulphide precipitate required by the present method should be homogeneous and finely divided. It is clear that as long as the two sulphides precipitate together and remain intimately mixed in the amorphous precipitate, the hydrogen reduction step appears to be sufficient to bring about alloy formation. Under the conditions of our preparation, the sulphides of platinum and ruthenium are PtS_2 and RuS_2, respectively. They are not isomorphous, PtS_2 having a $Cd(OH)_2$-type structure and the RuS_2 having a pyrite-type structure, but this difference, which is important in crystalline phases, does not seem to prevent the formation of a homogeneous, amorphous precipitate. This is also true for the Pt–Rh and Pt–Pd precipitates and alloys. On the other hand, in systems where the rates of precipitation of the two sulphides are very different, the intermediate precipitate will be heterogeneous and alloy formation will be difficult at low temperatures. This was evident in the preparations of Pt–Sn alloys, where the sulphide precipitation method could be applied with only limited success.

Finally, we have also carried out preliminary experiments to examine the catalytic activity of alloys prepared by the precipitation method. A solution containing H_2PtCl_6 and $RhCl_3$ was added to an alumina sol and treated with H_2S, thereby causing precipitation to take place on the alumina. The product was dried and fired at 500°C, in air, to yield a Pt–Rh/Al_2O_3 powder (the alumina having a surface area of approximately 100 m^2g^{-1}). This material was found to be catalytically active for a series of reactions, including the oxidation of carbon monoxide and propane. The work will be described in detail in a future publication.

ACKNOWLEDGMENTS

We thank Dr. A. J. Skarnulis and Mrs. A. E. Stoker for technical assistance and AERE Harwell for an EMR grant to one of us (A.J.S.C.). We gratefully acknowledge Dr. G. Butler and Mr. P. S. Drew of AERE Harwell for their assistance in this project.

REFERENCES

1. Adams, R., and Schriner, L., *J. Amer. Chem. Soc.* **45,** 2171 (1923).
2. Brown, H. C., and Brown, C. A., *J. Amer. Chem. Soc.* **84,** 1493 (1962).
3. Hall, W. K., and Emmett, P. H., *J. Phys. Chem.* **62,** 816 (1958). Best, R. J., and Russell, W. W., *J. Amer. Chem. Soc.* **76,** 838 (1954).
4. Cheetham, A. K., *Nature (London)* **288,** 469 (1980).
5. Cheetham, A. K., and Chowdhury, A. J. S., Proc., 10th Plansee Seminar **3,** 135, Metallwerk Plansee GMBH, Reutte, Austria, 1981.
6. Blanchard, G., Charcosset, H., Guenin, M., and Tournayan, L., *Surf. Sci.* **106,** 509 (1981).
7. Hutchinson, J. M., *Platinum Met. Rev.* **16,** 88 (1972).
8. Raub, E., and Falkenberg, G., *Z. Metallkd.* **55,** 392 (1964).
9. Raub, E., *J. Less-Common Met.* **1,** 3 (1959).
10. Harrison, B., Cooper, B. J., and Wilkins, A. J. J., *Platinum Met. Rev.* **25,** 14 (1981).
11. Cliff, G., and Lorimer, G. W., *J. Microsc. (Oxford)* **103,** 203 (1975).
12. Cheetham, A. K., and Skarnulis, A. J., *Anal. Chem.* **53,** 1060 (1981).
13. Wold, A., Arnott, R. J., and Croft, W. J., *Inorg. Chem.* **2,** 972 (1963).
14. Schmidt, L. D., Wang, T., and Vacquez, A., *Ultramicroscopy* **8**(1,2), 175 (1982).
15. Bouwman, R., and Sachtler, W. M. H., *J. Catal.* **26,** 63 (1972).
16. Jaffee, R. I., Maykuth, D. J., and Douglas, R. W., *in* "Refractory Metals and Alloys: Meta. Soc. Conf., Detroit, Vol. 11, 1960" (M. Semcheyshen and J. J. Harwood, Eds.), p. 419. Interscience, New York, 1961.
17. Sachtler, W. M. H., and Dorgelo, G. J. H., *J. Catal.* **4,** 654 (1965); Sachtler, W. M. H., and Jongepier, R., *J. Catal.* **4,** 665 (1965).
18. Bouwman, R., and Sachtler, W. M. H., *J. Catal.* **19,** 127 (1970).
19. NBS *Tech. Note (U.S.)* **270** (No. 1–6), 4–93 (1965).
20. Solliard, C., and Buffat, Ph., *J. Phys. Colloq.* C2, Supl. No. 7, 167 (1977).
21. Stoneham, A. M., *J. Phys. C,* Solid State Physics, **10,** 1175 (1977).
22. Temkin, D. E., *Sov. Phys.–Solid State (Engl. Transl.)* **11,** 27 (1970).